THE ASTROPHYSICAL JOURNAL, 301:571–586, 1986 February 15

BIPOLAR HYDROMAGNETIC WINDS FROM DISKS AROUND PROTOSTELLAR OBJECTS

RALPH E. PUDRITZ[1] AND COLIN A. NORMAN[1,2]
Received 1985 March 4; accepted 1985 August 20

ABSTRACT

The bipolar outflows associated with protostars are modeled as two-component, hydromagnetic winds which originate in the envelopes of rotating, magnetized molecular disks. We show that the torques exerted upon disks by centrifugally driven winds can account for both the observed linear momentum and energy transport rates associated with the molecular outflows. The prediction is that the luminosity associated with protostellar objects during the molecular outflow epoch is due to accretion from these disks. Massive molecular winds are synonymous with the main accretion epoch for stars with $M \gtrsim 1\ M_\odot$. These outflows can solve the angular-momentum problem of star formation and drive accretion onto the protostellar cores. The highly ionized component of the disk wind originates from disk radii $r \leq 10^{15}$ cm, at a mass loss rate $\dot{M}_{\rm ion} \sim 10^{-6}\ M_\odot\ {\rm yr}^{-1}$ and a terminal speed $V_{\rm ion} \approx 230$ km s^{-1}. Herbig-Haro (HH) objects are associated with this component. At radii $10^{15} \leq r \leq 10^{17}$ cm, the molecular flow originates from a cool neutral disk envelope, with a mass loss rate $\dot{M}_{\rm molec} \approx 10^{-4}\ M_\odot\ {\rm yr}^{-1}$ and a terminal speed $V_{\rm molec} \approx 50$ km s^{-1}. The lobes of high-speed CO are where this molecular wind reaches terminal speed. This molecular outflow produces a magnetohydrodynamic (MHD) shock as it collides with ambient molecular cloud gas with characteristic H_2 emission produced in the preshock region beyond the high-speed CO. Calculations are presented for the masses, rotation rates, and densities, and outflow characteristics for disks and their outflows, for the sources HH 7–11 (SVS 13), Orion–KL (IRc2), L1551 (IRS 5), and B335. FU Orionis–type outbursts can be accommodated naturally in our model when the molecular disks and winds are highly evolved and near the end of the accretion phase. The observational test for the centrifugal acceleration mechanism for all molecular outflows is to observe the outflowing gas corotating with the underlying disk out to the Alfvén surface on scales ≥ 0.2 pc.

Subject headings: galaxies: nuclei — hydromagnetics — stars: pre–main-sequence — stars: winds

I. INTRODUCTION

Energetic, bipolar, molecular outflows have been discovered in regions of star formation as diverse as the Orion–KL nebula and Bok globules. Radiative drives cannot explain the enormous observed rates of linear momentum transport ($\dot{M}_w V_w$) associated with these outflows. Thus, in all cases, $(\dot{M}_w V_w)/(L_*/c)$ is observed to be $\geq 10^2$, and for many it is $> 10^3$! We suggested earlier that these outflows were centrifugally driven, hydromagnetic winds from *disks* in which the protostars are embedded (Pudritz and Norman 1983, hereafter PN). The basic point of this model is that winds from fast magnetic rotators are extremely efficient in extracting angular momentum and rotational energy from the underlying rotating magnetized body. Gas is accelerated because the magnetic field enforces its corotation with the disk out to relatively large distances, so that cold outflows with very high terminal wind speeds can be established.

Why should disks rather than fast-rotating central stars (as in Hartmann and MacGregor 1982 and Draine 1983) be invoked as the underlying rotor? The important clue here is that in order to provide the molecular outflow with the observed rate of linear momentum transport, a stellar wind at 200 km s^{-1} would require a mass loss rate of at least $10^{-6}\ M_\odot\ {\rm yr}^{-1}$. Recent observations of the T Tauri source by Knapp and Padgett (1985) show, however, that whereas the molecular outflow requires at least $\dot{M}_{\rm star} \gtrsim 4 \times 10^{-6}\ M_\odot\ {\rm yr}^{-1}$, the upper limit on stellar mass loss derived from VLA measurements of the 5 GHz radio continuum flux (Cohen, Bieging, and Schwartz 1982) is $\dot{M}_{\rm star} \lesssim 1.6 \times 10^{-7}\ M_\odot\ {\rm yr}^{-1}$. Thus, a stellar wind is ruled out as the drive for at least those molecular outflows for which radio continuum measurements are available. Disks are an attractive source of the wind because their surface gravity is much smaller than that of the protostellar core. Winds from magnetized, rotating disks can remove angular momentum and allow growth of a central protostar which has very low specific angular momentum. Star formation in protostellar disks may be regulated by a process in which accretion through the disk and onto the protostellar core is determined by the rate at which angular momentum can be extracted by a hydromagnetic disk wind (Pudritz 1985).

Hydromagnetic disk winds carry off the excess angular momentum of gas in the disk, and drive the accretion of low specific angular momentum material onto a central object. In comparison with thermal or radiatively driven winds, hydromagnetic winds have long lever arms. The advantage here is that a single test particle, forced to corotate with the underlying disk by the open field line which it follows, carries off not only its own angular momentum but also that of the disk it is leaving behind. This is quite different from thermally driven winds (e.g., Begelman, McKee, and Shields 1983), where a particle can really carry off only its own angular momentum. One cannot brake such a system because to do so means simply to drive off the whole disk. For hydromagnetic winds which are Poynting flux–dominated (fast magnetic rotators [FMRs]; Belcher and MacGregor 1976), efficient braking occurs with wind mass loss rates $\dot{M}_w \ll \dot{M}_a$. Those hydromagnetic winds from slowly rotating bodies (the Sun is a good example) which are

[1] Department of Physics and Astronomy, Johns Hopkins University.
[2] Space Telescope Science Institute, Johns Hopkins University.

denoted as slow magnetic rotators (SMRs) can brake efficiently only at wind mass loss rates of $\dot{M}_w \sim \dot{M}_a$; and, clearly, thermally and radiatively driven winds cannot act as brakes in accretion flows other than by simply evaporating the whole disk anyway.

In this paper we show that the hydromagnetic torque that a wind exerts on its underlying disk gives a straightforward explanation not only of the wind momentum flow $[(\dot{M}V)_w \gtrsim (10^2\text{–}10^3)(L_*/c)]$ but of the observed wind energetics as well. We show in §§ II*d* and II*e* that the observations are readily explained if disk winds are operative and if the luminosity associated with the embedded IR sources arises by *accretion* (driven by the wind) onto a protostellar core, rather than by nuclear burning. We build up a general picture of winds from disks (§ II*g*) which features (1) a molecular outflow of material from disk radii $r \gtrsim 10^{15}$ cm and (2) an ionized-gas outflow of disk material at disk radii $r \lesssim 10^{15}$ cm.

The ionized inner region produces the radio continuum emission seen at the VLA, and we propose that the optical and radio jets sometimes observed to be associated with young stellar objects are the cores of much more extended winds. HH objects are shown to be associated with this component. In molecular outflows, it is emphasized that molecular gas is accelerated from the disk envelope (on $\sim 10^{16}$ cm scales) and achieves terminal speeds on $\sim 10^{17}$ cm scales. The explanation of the so-called high-velocity CO lobes is that this is the scale on which the molecular outflow reaches terminal velocity. Observations ought to show, then, that streaming CO gas is spatially distributed and that intermediate velocities are to be found between the disks and the high-speed lobes (see also Uchida and Shibata 1985). This is quite different from the picture of CO emission associated with a stellar-wind–driven shell of ambient molecular gas.

In § III we discuss the application of disk winds to T Tauri stars while they are still embedded in the molecular cloud. This stage is of interest because it bridges the gap between young objects which are associated with massive molecular outflows, and the rather more pristine environments of those T Tauri stars which are certainly undergoing nuclear burning. In §§ IV and V we discuss a new theory for FU Orionis phenomena which may arise in the last stages of the accretion phase. In this phase the inner disk becomes Keplerian while the outer disk is still self-gravitating. With this structure, disk winds drive different accretion rates through these zones, resulting in mass accumulation at the outer edge of the Keplerian zone. Instabilities in this region could give bursts of accretion onto the core. Finally, in § VI we make detailed predictions about the observed disk and outflow properties for the objects Orion–KL (IRc2), NGC 7538, L1551 (IRS 5), and HH 7–11 (SVS 13).

II. WIND TORQUES ON DISKS AND BIPOLAR OUTFLOW CHARACTERISTICS

We assume that disks are threaded by generally open field lines which tend to parallel the rotation axis, and adopt a model of the magnetic flux diverging as some power of the cylindrical radius, here denoted r (PN).

a) Basic Features of Hydromagnetic Winds

A straightforward generalization of Bernoulli's theorem to dissipationless magnetized flows shows that the energy density of the flowing gas,

$$E = \frac{1}{2}(v_p^2 + v_\phi^2) + \frac{s^2}{\gamma - 1} - \psi - \frac{v_\phi A_p A_\phi}{v_p} = \text{const}\,, \qquad A_{p,\phi} \equiv b_{p,\phi}(4\pi\rho)^{-1/2}\,, \tag{2.1}$$

is a constant along streamlines, where s is the sound speed ($s = dp/d\rho$) for a polytropic index γ; ψ is the gravitational potential; and the subscript p, ϕ denotes poloidal (toroidal) quantities. The last term in equation (2.1) is directly related to the Poynting flux associated with the open, rotating field. The second quantity required to analyze hydromagnetic winds is the total specific angular momentum along a field line. For frictionless flows, the conserved transverse angular momentum is comprised of a material and magnetic part (the latter because twisted fields transport angular momentum):

$$l = r\left(v_\phi - \frac{A_p A_\phi}{v_p}\right) = \text{const}\,. \tag{2.2}$$

These two conserved quantities together with the mass flow rate along field lines are the essential features of the energy equation and the equations of continuity and motion. The induction equation for the field shows that the toroidal and poloidal fields are simply related; that is,

$$b_\phi/b_p = (v_\phi - \Omega r)/v_p\,, \tag{2.3}$$

where Ω is the rotation frequency of the central rotor to which the field lines are attached and with which they corotate.

The solution of equations (2.2) and (2.3) shows that there is a critical point in the flow at the Alfvénic point ("lever arm" length) which determines the value of l:

$$l = \Omega r_A^2\,, \tag{2.4}$$

where r_A is the Alfvén radius (where $b_p^2/4\pi = \rho v_p^2$). At radii $r \gg r_A$ the field is unable to force the gas to corotate with the disk so that $v_\phi \sim r^{-1}$. Magnetic acceleration really occurs between the slow point and this Alfvén radius, and the outflow acquires terminal poloidal speeds of order $v_p \sim \Omega r_A$. A long lever arm [$r_A(r) \gg r$], therefore, ensures acceleration to high terminal velocities. If a field line threads the disk surface at radius r_0 and makes an angle θ_0 with it, then the magnetic flux Φ_0 and wind mass loss rate $\dot{M}_w$ are modified to $\Phi_0' \equiv \Phi_0 \sin\theta_0$ and $\dot{M}_w' \equiv \dot{M}_w \sin\theta_0$, respectively. Blandford and Payne (1982) give a detailed treatment of non-equatorial centrifugally driven winds, solved for a self-similar model.

The magnetic flux per steradian $\Phi = b_p r^2$, and the mass flux $\dot{M}_w \equiv 4\pi\rho v_p r^2$, are conserved quantities. The terminal speed of a

cold magnetohydrodynamic (MHD) wind is of order (Michel 1969)

$$V_\infty \sim V_M = \left(\frac{\Omega^2\Phi^2}{\dot{M}_w}\right)^{1/3} \qquad \text{(cold outflows)}\,, \tag{2.5}$$

so that to within factors of order unity, the Alfvén radius is of order

$$r_A \approx \frac{V_M}{\Omega} = \left(\frac{\Phi^2}{\Omega\dot{M}_w}\right)^{1/3}\,, \tag{2.6}$$

where the detailed numerical factor depends upon the geometry of the poloidal field. (This factor is 3/2 for a monopolar, equatorial wind, and the outflow speed has attained $\frac{2}{3}V_M$ at this radius.) We anticipate that the corrections to equations (2.5) and (2.6) that arise for polar outflows are that $\Phi \rightarrow \Phi'$ and $\dot{M}_w \rightarrow \dot{M}'_w$ (see Blandford and Payne 1982, eq. [2.7b]).

The energy equation (2.1) then shows that in the limit $r \rightarrow \infty$, the constant E takes the value

$$E = \frac{1}{2}V_\infty^2 + \frac{V_M^3}{V_\infty} \tag{2.7}$$

which says that the material at terminal speed V_∞ contributes its kinetic energy and the field its Poynting flux to the total energy loss from the central rotor. In the absence of rotation, of course, $V_M = 0$ (no toroidal field b_ϕ) and equation (2.7) is a quadratic rather than a cubic equation for the matter's terminal speed V_∞ (the Parker speed):

$$\frac{1}{2}V_\infty^2 \equiv \frac{1}{2}V_P^2 = \frac{s_0^2}{\gamma - 1} - \psi_0 + \frac{v_{p,0}^2}{2}\,, \tag{2.8}$$

where a subscript zero denotes a value on the disk.

In the limit in which rotation is dominant, one is in the FMR regime ($V_M \gg V_P$), and where rotational effects are small, in the SMR regime ($V_P \ll V_M$) with asymptotic wind velocity

$$\begin{aligned} V_\infty &\sim V_M \qquad \text{(FMR)} \\ &\sim V_P \qquad \text{(SMR)}\,. \end{aligned} \tag{2.9}$$

These two regimes correspond to the case when energy loss is predominantly carried by the field (FMR), or by warm gas channeled by the field (SMR) (Belcher and MacGregor 1976).

The torque that an outflowing wind, forced to corotate with an underlying disk, must exert upon the disk is

$$T_w = -\dot{J}_{\text{disk}} = \int l\rho \boldsymbol{v}_{\rho,w} \cdot d\boldsymbol{A} \approx f_g \dot{M}_w \Omega r_A^2\,, \tag{2.10}$$

where the integral is being taken over the locus of all Alfvén points on individual field lines (the surface $\boldsymbol{A}$). This expression assumes that mostly open magnetic field lines thread the disk. A factor of order unity (f_g) appears in equation (2.10) which arises from the detailed geometric structure of the poloidal field (the factor f_g is equal to $\frac{2}{3}$ for monopolar, equatorial winds, and $\frac{1}{3}$ [Pudritz 1985] for monopolar, "polar" winds).

b) Magnetic Field Geometry

The key assumption implicit in writing the torque (2.10) is that the flux threading the molecular disk is open and takes on an "hourglass" configuration as diagrammed in Figure 1. The reason that this geometry is used is twofold. The formulation of molecular disks may well involve preferential contraction of gas along, as opposed to across, field lines. Observations of bipolar outflows, where magnetic field orientation via polarization measurements can be inferred, shows that in half the cases, outflow and magnetic field axes are aligned to within $\sim \pm 20°$ (see Cohen, Rowland, and Blair 1984). Detailed study of the magnetic field structure of an isolated Bok globule shows very convincing evidence for such a field geometry (Jones, Hyland, and Bailey 1984). Polarimetry at 2.3 μm for nine infrared sources associated with bipolar outflows shows large linear polarizations with position angles perpendicular to the outflow direction (Sato *et al.* 1985), indicating the presence of dusty disks in these planes.

Mestel (1968) and Roxburgh (1983) consider stellar hydromagnetic wind torques. If the central star has fields more complicated than monopolar (Mestel considered dipolar geometry and Roxburgh general n-pole fields), then the integral in equation (2.10) can be taken only over those flux tubes that are open to infinity. By modeling the true flow plus field geometry as an n-pole out to r_A and a radial (monopolar) outflow beyond, these authors indicated that more complicated dependences of T_w upon r_A would obtain for stellar outflows.

We model the threading disk field as an open interstellar field that is trapped in a contracting disk so that a monopolar geometry is the relevant one. The point is that it is a disk wind, not a protostellar wind, which is hypothesized to be the drive for bipolar outflows. Closed magnetic structures for disks could arise if significant turbulent dynamo action were to occur (see Pudritz 1981), but whether this is possible in the molecular disks under discussion is an open question. It is to be expected that the polar outflow pictured in Figure 1 has significant gradients of toroidal magnetic field in the wind, and Sakurai (1985) has shown that such stresses can collimate centrifugal winds. We would expect important deviations from formula (2.10) in the case of highly collimated polar outflow.

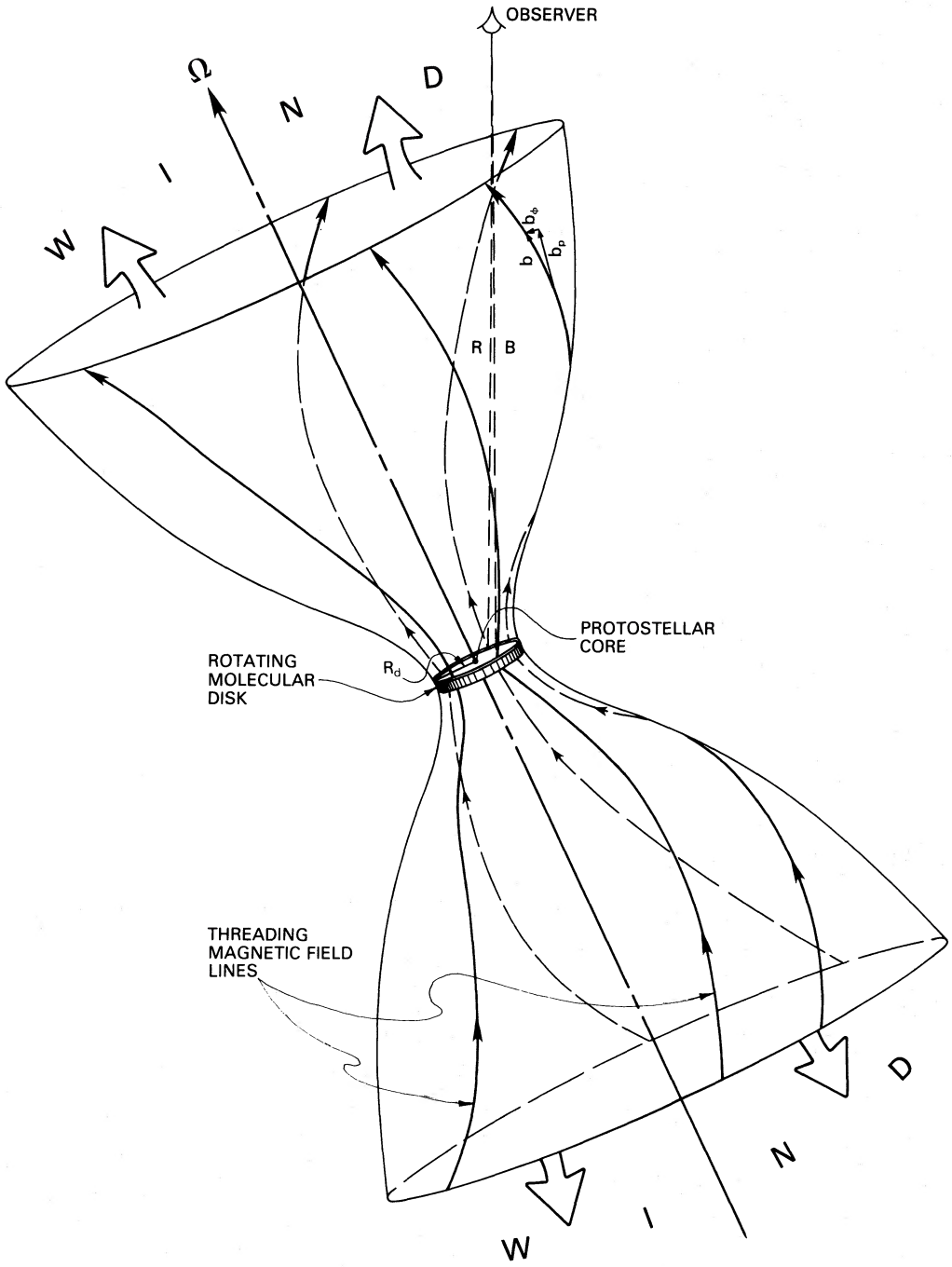

FIG. 1.—Observing a bipolar hydromagnetic disk wind. Pictured here is a sheet of accelerating molecular gas which originated at a radius r in the envelope of a molecular disk in which a protostellar core is growing. The magnetic field which threads the disk at r is strong enough to force the gas to corotate with the disk out to roughly the Alfvén radius $r_A(r)$. This enforced corotation is what accelerates the gas to form a bipolar wind. As $r_A(r)$ is approached, the field becomes increasingly toroidal. Far beyond the wind fast point, the toroidal field dominates and provides a "hoop stress" which collimates the outflow. The *observational test of the acceleration mechanism* is to look for a characteristic signature of rotating gas in the bipolar outflow. At distances $R \gg r_A(r)$, the toroidal speed of the accelerating gas falls as $V_\phi(R) \propto R^{-1}$. For $R \leq r_A(r)$, however, the accelerating gas corotates with the disk. Therefore, superposed upon the broad-line shape due to the poloidal gas speed, there is some asymmetry due to the corotation of the accelerating gas. In the figure, emission from the lines of sight $B(R)$ are slightly blueshifted (redshifted). Of course, this effect varies with viewing angle.

c) Wind-induced Accretion in Disks

The disk angular momentum equation is, in steady state, just

$$\frac{\dot{M}_a}{2\pi r^2}\frac{d}{dr}(ru_\phi) = \frac{1}{r^2}\frac{d}{dr}(r^2\langle\sigma_{\phi r}\rangle) + \left\langle\frac{\partial\sigma_{\phi,z}}{\partial z}\right\rangle, \tag{2.11}$$

where u_ϕ is the toroidal speed of disk material, $\dot{M}_a = \langle 2\pi\rho v_r r\rangle$ is the disk accretion rate, $\sigma_{\phi,r}$ and $\sigma_{\phi,z}$ are the torques per unit area exerted by the stress $\boldsymbol{\sigma}$, and the angular brackets denote vertical averaging. This expression shows that the gas can accrete at the rate at which the radial ($\sigma_{\phi,r}$) and vertical ($\sigma_{\phi,z}$) stresses can remove angular momentum. A hydromagnetic bipolar wind induces a significant stress across the disk's upper and lower surfaces, thereby extracting angular momentum and rotational energy. If σ is the Maxwell stress and if the field through the disk is predominantly vertical, then only the second term on the right-hand side of equation (2.11) is important, with the result (using eq. [2.10]; see Pudritz 1985)

$$\dot{M}_a\frac{d}{dr}(ru_\phi) = \frac{d}{dr}(f_g\dot{M}_w\Omega r_A^2). \tag{2.12}$$

This expression shows that in any portion of the disk where hydromagnetic stresses are responsible for driving an accretion flow at the rate $\dot{M}_a$, one has (integrating eq. [2.12])

$$\dot{M}_a r^2 = f_g\dot{M}_w r_A^2(r). \tag{2.13}$$

Equation (2.13) states that, in steady state flows, there is a balance of the moments of inertia between the inflowing disk material and the column of outflowing wind forced to corotate with the disk below. Notice that in the limit $r_A \gg r$, a tiny wind outflow drives a much larger accretion rate.

A viscous torque spreads out the material from an annulus in both inward and outward radial directions, with most of the mass moving inward and an ever decreasing number of particles moving outward and carrying off the angular momentum of their companions (von Weizsäcker 1943; Lüst 1952; Lynden-Bell and Pringle 1974). The wind mechanism of angular-momentum transport causes a torus to move steadily inward, with a small portion of its mass being accelerated out to infinity in polar directions.

d) An Explanation for the Momentum Transport Rate in Bipolar Winds

There is a simple explanation for the fact that $\dot{M}_w V_w/(L/c) \gtrsim 10^3$ in bipolar flows. The basic point is that a hydromagnetic disk wind drives accretion at the rate given by equation (2.13). Thus, if the accretion rate $\dot{M}_a$ onto a core of mass $M_{\rm core}$ and radius $R_{\rm core}$ occurs, the associated luminosity is just

$$L = \epsilon G\dot{M}_a M_{\rm core}/R_{\rm core}, \tag{2.14}$$

where $\epsilon \approx 1 - (\Omega_{\rm core}R_{\rm core}/V_{\phi,d})$ is an efficiency factor which depends upon the relative rotation of the stellar core and the abutting disk (e.g., Pringle 1977). We believe that $\epsilon \approx 0.1$, but caution that a detailed boundary-layer calculation is needed in order to find an accurate value.

Hence, using equation (2.14) as the effective luminosity of the central source, and using equation (2.13) to eliminate M_w in favor of $\dot{M}_a$, one finds

$$\frac{\dot{M}_w V_w}{L/c} = \frac{2}{\epsilon f_g}\left(\frac{r}{r_A}\right)^2\frac{V_w}{c}\left(\frac{R_{\rm core}}{R_{\rm Schw}}\right), \tag{2.15}$$

where $R_{\rm Schw} = 2GM_{\rm core}/c^2$ is just the Schwarzschild radius for the core mass. If the approximate result that $V_w \sim V_M \sim \Omega R_A$ is used, then the formula

$$\frac{\dot{M}_w V_w}{L/c} \approx \frac{2}{\epsilon f_g}\left(\frac{\Omega r}{c}\right)\left(\frac{r}{r_A}\right)\left(\frac{R_{\rm core}}{R_{\rm Schw}}\right) \tag{2.16}$$

$$\approx 108\left(\frac{0.33}{\epsilon f_g}\right)\left(\frac{R_d/R_A}{10^{-1}}\right)\left(\frac{R_{\rm core}}{10^{12.5}\ {\rm cm}}\right)\left(\frac{M_\odot}{M_{\rm core}}\right)\left(\frac{V_{\rm rot}}{5\ {\rm km\ s^{-1}}}\right) \tag{2.17}$$

is obtained for the momentum flow in winds originating from molecular disks. Notice that, since R_A marks the typical scale on which gas reaches terminal speed, high-speed CO lobes will appear on scales $R_A \lesssim 10R_d$ or at fractions of a parsec. Thus, relation (2.17) also gives an explanation for the position of the highest speed molecular gas.

e) An Explanation for the Energetics of Bipolar Winds

Following the procedure of the previous section, the ratio of the mechanical luminosity of the disk outflow (assuming eqs. [2.14] and [2.13]) is

$$\frac{L_{\rm mech}}{L_*} \equiv \frac{1}{2}\frac{\dot{M}_w V_w^2}{L_*} = \frac{1}{\epsilon f_g}\left(\frac{V_{\rm rot}}{c}\right)^2\left(\frac{R_{\rm core}}{R_{\rm Schw}}\right). \tag{2.18}$$

As an aside, it is useful to note that $L_{\rm mech}$ derives from the release of gravitational binding energy of the accreting disk gas; i.e.,

$L_{\rm mech} \approx (2\epsilon f_g)^{-1} \dot{M}_a V_{\rm rot}^2$. The point here is that the magnetic wind torque efficiently converts gravitational energy release during accretion, to ordered outflow.

The result (2.18) is important because it predicts the relation between the *observed ratio* $(L_{\rm mech}/L_*)$ and the rotation of the underlying disk to be

$$\frac{V_{\rm rot}}{5\ {\rm km\ s^{-1}}} = 1.07\left[\left(\frac{\epsilon f_g}{0.33}\right)\left(\frac{M_{\rm core}}{M_\odot}\right)\left(\frac{R_{\rm core}}{10^{12.5}\ {\rm cm}}\right)^{-1}\right]^{1/2}\left(\frac{L_{\rm mech}/L_*}{10^{-2}}\right)^{1/2} . \tag{2.19}$$

These values of $V_{\rm rot}$ for molecular disks are consistent with the observation rotation velocities presently ascribed to molecular disks. It is interesting to note that when high-resolution observations determine $V_{\rm rot}$ and $(L_{\rm mech}/L_*)$ for flows off disks, then equation (2.19) shows that the ratio $M_{\rm core}/R_{\rm core}$ is uniquely determined. The fact that $(L_{\rm mech}/L_*) \sim 10^{-2}$–$10^{-3}$ for most outflows stems naturally from the fact that maximum energy release occurs during accretion onto the protostellar core.

f) Comparison with Viscous Torques

The "viscous" stress acting in a turbulent accretion disk was modeled in a very simple way by Shakura and Sunyaev (1973). If the coefficient of kinematic viscosity ν is written as $\nu = \alpha c_d z_d$, where c_d and z_d are respectively the disk sound speed and half-thickness and α is taken to be a constant $\lesssim 1.0$, then the viscous torque that acts between orbiting annuli of gas may be written (Pringle 1981)

$$T_\nu = 2\pi r^2 m \nu \Sigma \Omega . \tag{2.20}$$

Here, m is a measure of the shear gradient in the disk; viz., $m \equiv d(\ln \Omega)/d(\ln r)$. Introducing a power-law form for the surface density allows equation (2.20) to be written as

$$T_\nu = \left(\alpha m n M_d \frac{c_d}{z_d}\right)\Omega z_d^2 , \tag{2.21}$$

where the disk mass $M_d(r)$ is $dM_d/dr = 2\pi r\Sigma$ and $n \equiv d(\ln M)/d(\ln r)$ is assumed to be a constant. Equation (2.21) shows that the lever arms of viscous torques are $\sim z_d$.

We compare the torques that hydromagnetic disk winds exert with possible viscous torques in the case of self-gravitating molecular disks. Since the isothermal scale height of such a disk is $z_d = c_d^2/\pi G\Sigma_d$, then we may write

$$\frac{c_d}{z_d} = \frac{\lambda}{Q}\Omega , \tag{2.22}$$

where Q is the fluid disk analog of the Toomre parameter ($Q = C_d \kappa/\pi G\Sigma_d$) and where $\kappa \equiv \lambda\Omega$ is the epicyclic frequency.

The ratio of wind to viscous torques may be formed by substituting equation (2.22) in equation (2.21) and employing equation (2.10), to find

$$\frac{T_w}{T_\nu} = \left(\frac{f_g Q}{\alpha m n \lambda}\frac{\dot{M}_w}{M_d \Omega}\right)\left(\frac{r_{\rm A}}{z_d}\right)^2 . \tag{2.23}$$

Recent observations have interpreted systematic velocity gradients across molecular disks as arising from rotation (e.g., Plambeck *et al.* 1985); and for disks of 7×10^{16} radius and 4 km s^{-1} rotation speed, $\Omega \sim 5 \times 10^{-12}$ s^{-1} is suggested (Pudritz 1985). Thus, with $\dot{M}_w$ and M_d already given ($10^{-4}\ M_\odot\ {\rm yr^{-1}}$ and $\lesssim 100\ M_\odot$, respectively), formula (2.23) shows that wind torques dominate when $(r_{\rm A}/r) \gtrsim 10(\alpha n m \lambda/Q f_g)^{1/2}(z_d/r)$. Under simple assumptions z_d/r may be shown to be of order ~ 0.2, in agreement with the present limited set of observed disk axial ratios. Therefore, even if $\alpha \sim 1$, a lever arm $r_{\rm A}/r \gtrsim 2$ will result in a dominant wind torque in the self-gravitating molecular disks under discussion.

g) An Integrated Model of Winds and Disks around Protostars

The accretion flow onto the protostellar core produces far-ultraviolet radiation in the optically thick accretion shock. The Lyman continuum photons from this accretion shock may entirely ionize gas in an inner disk envelope which extends to scales $R_{\rm en}^I \sim 10^{15}$ cm. The mass loss rate associated with this inner disk envelope can be shown to be (Pudritz 1985)

$$\dot{M}_{\rm ion} \approx 10^{-6} M_2^{-2} h_{22.5}^{8/3} Q_{47}^{2/3}\ M_\odot\ {\rm yr^{-1}} , \tag{2.24}$$

where $M_2 \equiv M_d/10^2\ M_\odot$ and $h_{22.5} = h/10^{22.5}$ cm^2 s^{-1} are the dimensionless disk mass and specific angular momentum, $Q_{47} \equiv (Q/10^{47}$ Lyman continuum photons s$^{-1})$, and where a factor which is extremely insensitive to core parameters has been neglected. The mass loss associated with *molecular gas outflow* from the neutral envelope at $R_{\rm en}^I \le r \le R_d$ is

$$\dot{M}_{\rm molec} \approx 0.82 \times 10^{-4} M_2^3 h_{22.5}^{-8/3} g(\theta = 15°)\ M_\odot\ {\rm yr^{-1}} , \tag{2.25}$$

where $g(\theta)$ is a function specifying the opening angle that field lines make with the disk (here $2\theta = 30°$). Factors which are insensitive to core parameters are suppressed. The terminal speed of the molecular gas is

$$V_{\infty,{\rm molec}} \approx 52 M_2 h_{22.5}^{-10/9} g^{2/3}(\theta = 15°)\ {\rm km\ s^{-1}} . \tag{2.26}$$

The molecular disk extends out to $R_d \sim 7 \times 10^{16} M_2^{-1} h_{22.5}^2$ cm and rotates at $V_\phi \approx 4 M_2 h_{22.5}^{-1}$ km s^{-1}. The large disk size arises because of the large specific angular momentum that the disks are observed to contain. Thus we see that the neutral mass loss rates

and terminal speeds are in the correct range observed for bipolar molecular flows, without any interpretation that $V_{\infty,\mathrm{molec}}$ is the velocity of a swept-up shell of gas. The ionized mass outflow is in line with VLA measurements of force-free emission at mJy flux levels. The terminal speed of ionized gas, which may later recombine, could also be centrifugally driven, so from equation (2.6*a*) we may write

$$\frac{V_{\infty,\mathrm{ion}}}{V_{\infty,\mathrm{molec}}} \approx \left(\frac{V_{\phi,\mathrm{ion}}}{V_{\phi,\mathrm{molec}}}\right)^{2/3}\left(\frac{[\Phi/r]_{\mathrm{ion}}}{[\Phi/r]_{\mathrm{molec}}}\right)^{2/3}\left(\frac{\dot{M}_{\mathrm{molec}}}{\dot{M}_{\mathrm{ion}}}\right)^{1/3} . \tag{2.27}$$

This formula can be evaluated in general with knowledge of the rotation curve and the flux distribution across the disk.

For a flat rotation curve and a flux distribution such that $\Phi \propto M_d \propto r$ (see § IV*b*), the terminal speed is larger than the molecular outflow, i.e.,

$$V_{\infty,\mathrm{ion}} \approx 226 M_2^{8/3} h_{22.5}^{-26/9} Q_{47}^{-2/9} g(\theta = 15^\circ)\ \mathrm{km\ s^{-1}} , \tag{2.28}$$

which can drive shocks. Therefore, if it is supposed that the disk extends into an AU with a flat rotation curve and $V_{\mathrm{rot}} = 5$ km s^{-1}, gas accelerated from this point achieves 230 km s^{-1} at $R_A \approx 6.8 \times 10^{14}$ cm. When significant protostellar mass has accumulated, the rotation curve near the core becomes Keplerian, so that much higher disk rotation and terminal wind speeds can be obtained. The combination of ionized gas outflow velocity (2.28) and mass loss rate (2.24) will be expected to produce a radio continuum flux of order $S_\nu \sim 4.4$ mJy at $\nu = 5$ GHz with electron temperatures of 10^4 K and distance to source of 500 pc assuming an electron density profile $n_e(r) \propto r^{-2}$ (Panagia and Felli 1975).

It is interesting to note how insensitive the foregoing results are to the flux of Lyman continuum photons. Thus, while variations in the acceleration rate may considerably alter this flux, the ion flow parameters do not drastically change. To see this, we note that $\dot{M}_{\mathrm{ion}} \propto 10^{-6} Q_{47}^{2/3}\ M_\odot\ \mathrm{yr^{-1}}$, $V_{\infty,\mathrm{ion}} \propto 226 Q_{47}^{-2/9}$ km s^{-1}, and $\dot{M}_{\mathrm{ion}} V_{\infty,\mathrm{ion}} \propto 2.26 \times 10^{-4} Q_{47}^{4/9}\ M_\odot\ \mathrm{yr^{-1}}$ km s^{-1}. As a concrete example, a variation of Q by 2 orders of magnitude ($Q = 10^{45}$ s^{-1}, say) results in $\dot{M}_{\mathrm{ion}} \rightarrow 4.6 \times 10^{-8}\ M_\odot\ \mathrm{yr^{-1}}$, $V_{\infty,\mathrm{ion}} \rightarrow 629$ km s^{-1}, and $\dot{M}_{\mathrm{ion}} V_{\infty,\mathrm{ion}} \rightarrow 2.92 \times 10^{-5}\ M_\odot\ \mathrm{yr^{-1}}$ km s^{-1}. It is important to realize that a drop in the ionized mass loss rate actually increases $V_{\infty,\mathrm{ion}}$ (see eq. [2.27]), although of course the torque exerted by and the thrust of this component would be reduced. Herbig-Haro objects require shock velocities of ≥ 200 km s^{-1} (Schwartz 1983), and the previous remark makes it clear that this occurs for $\dot{M}_{\mathrm{ion}} \leq 10^{-6}\ M_\odot\ \mathrm{yr^{-1}}$ (i.e., $Q_{47} \leq 1$). Central outflows more massive than this could not drive the HH phenomenon.

Gathering together these points about core outflows allows an *explanation of HH objects.* They must in our picture be associated with the inner-core outflow when it achieves a mass loss rate of order $10^{-6}\ M_\odot\ \mathrm{yr^{-1}}$. Notice that because the inner and outer (molecular) flows achieve different terminal speeds, the relative shear between the two components will become large enough at some point in the outflow that Kelvin-Helmholtz instabilities will develop (see, e.g., Königl 1982). When this happens, clumps of molecular material (moving at 50 km s^{-1}) will be torn off the interface between the two outflows, and shocked in the inner wind (moving at 250 km s^{-1}) at shock velocities of ~ 200 km s^{-1}.

We give a sketch of the integrated model in Figure 2, which pictures the formation of a massive star. A massive molecular disk drives off a two-component wind (an inner ionized and outer molecular component) at typical mass loss rates of $\dot{M}_{\mathrm{ion}} \sim 10^{-6}\ M_\odot\ \mathrm{yr^{-1}}$ and $\dot{M}_{\mathrm{molec}} \sim 10^{-4}\ M_\odot\ \mathrm{yr^{-1}}$. The massive molecular outflow is accelerated up to terminal speed on scales of fractions of a parsec in size. Then high-speed CO lobes are at the approximate position of the Alfvénic surface R_A in these winds. The molecular outflow is the most extensive, and shocks the ambient molecular cloud at the MHD shock front. Shocked molecular hydrogen and other shocked species originate beyond this surface (see, e.g., Draine and Roberge 1982). High-speed core gas may be responsible for shocking inhomogeneities in this inner core to produce Herbig-Haro objects. A flux of the order of several mJy is expected in the radio continuum. The massive molecular wind is primarily responsible for driving an accretion flow through the disk at rates up to $\dot{M}_a \approx 10^{-3}\ M_\odot\ \mathrm{yr^{-1}}$ (see Pudritz 1985). The momentum and energy carried by the molecular outflow is accounted for if the luminosity of the central source is due to accretion (see §§ II*d* and II*e*). The general "hourglass" configuration of the field and the outflow it guides is due to the radial contraction of the disk due to gravitation. The entire outflow is magnetically collimated by "hoop stress" generated by the wind's toroidal field. Blandford and Payne (1982) developed a self-similar model for hydromagnetic disk winds. We have suggested (Pudritz and Norman 1986) that more general disk models than theirs would also admit self-similar wind solutions.

III. EMBEDDED T TAURI STARS: WINDS, DISKS, AND EVOLUTION

a) Winds

Edwards and Snell (1984) have made a survey for high-velocity CO gas toward 49 Herbig-Haro objects and have found 11 identified bipolar outflows in the vicinity. The majority of the 32 HH objects in the vicinity of these 11 flows are at the periphery or beyond the boundaries of these outflows. Bieging, Cohen, and Schwartz (1984) have surveyed the T Tauri stars in the Taurus-Auriga cloud for 5 GHz radio continuum emission and found that the T Tauri stars which excite HH objects are much more likely to have detectable radio emission than those not associated with HH objects. The reason for this observation in our picture is that the HH phenomenon starts only when the inner region has $M \leq 10^{-6}\ M_\odot\ \mathrm{yr^{-1}}$ (§ II*g*). This corresponds to a density low enough for the gas to be kept hot by the ionizing flux. Mundt and Fried (1983) have discovered optical-jet–like emission from DG Tau, HH 30, HC Tau, and IRS 5 in L1551 and indicate that their collimation must take place at distances smaller than 3×10^{15} cm.

Recent observations by Knapp and Padgett (1985) show that the region of high-speed CO outflow around T Tau is larger than previously found (see Edwards and Snell 1984), making $(\dot{M}V)_w$ even larger for this molecular outflow. The measurements of resonance Na D lines for T Tau (Ulrich and Knapp 1985) show that an outflow associated with the central star is $V \sim 200$ km s^{-1}. If the stellar wind is to push the CO outflow, then a high $\dot{M}_*$ is required. In fact, using the measured radio continuum flux of ~ 5.8 mJy (Cohen, Bieging, and Schwartz 1982) Knapp and Padgett (1985) conclude that $\dot{M}_* \lesssim 1.6 \times 10^{-7}\ M_\odot\ \mathrm{yr^{-1}}$. However, momentum balance for the outflow requires $\dot{M}_w \gtrsim 4 \times 10^{-6}\ M_\odot\ \mathrm{yr^{-1}}$. This large discrepancy can be readily accounted for by a molecular outflow from a disk in which the star is still embedded.

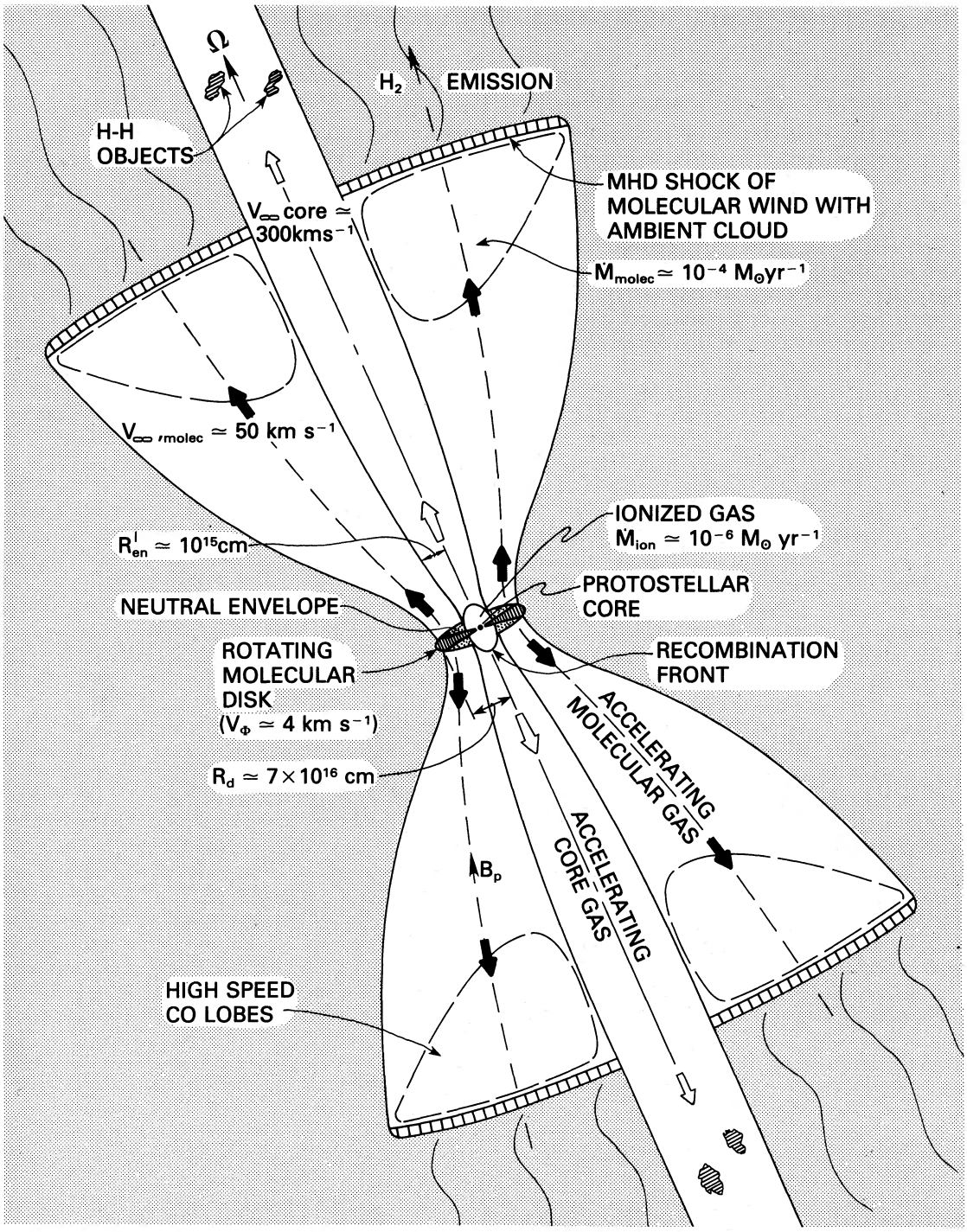

FIG. 2.—A unified model for outflows and disk around protostars. A massive protostar is forming in a massive ($\sim 10^2\ M_\odot$) molecular disk, rotating at ~ 4 km s^{-1}. A hydromagnetic wind blows off the disk, carrying away its angular momentum and driving accretion onto the protostellar core. At radii $R^I_{en} \sim 10^{15}$ cm $\lesssim R \lesssim R_d \sim 7 \times 10^{16}$ cm, a molecular outflow, originating from a cool neutral envelope, is accelerated up to terminal speed of ~ 50 km s^{-1} at a scale $R_A \sim 0.3$ pc, with a mass loss rate $M_{molec} \sim 10^{-4}\ M_\odot$ yr^{-1}. This molecular wind collides with ambient molecular cloud material (*shaded region*), causing an MHD shock and a lobe of H_2 emission beyond the high-speed CO lobe. Inside disk radii $r \leq 10^{15}$ cm, Lyman continuum from the accretion shock ionizes a core envelope and results in $\dot{M}_{ion} \sim 10^{-6}\ M_\odot$ yr^{-1} at $V_{ion} \sim 200$ km s^{-1}. This outflow remains ionized for low mass loss rates and is the component identified by VLA and optical observations. Near the disk, OH masers appear near R^I_{en}; and far down the flow, HH objects are driven by the core component of the overall disk wind. HH objects may result by Kelvin-Helmholtz instability between the fast core gas and the slower-moving molecular outflow.

Another point to consider about mass outflow from stars versus circumstellar disks is the energetics driving the Herbig-Haro objects. For HH I and HH II, Mundt and Hartmann (1983) note that in order to shock these objects with at least a 100 km s^{-1} wind, and to provide the mechanical luminosity of $L_{HH} \approx 7.5\ L_\odot$, a mass loss of $\dot{M} \sim 10^{-6}$ ought to be ascribed to the wind. This is again a large value in comparison with observations of the central stars. Since HH objects, radio continuum emission, and CO outflows appear to be still connected for embedded T Tauri stars, we suggest that mass loss from surrounding disks can solve these problems.

Optical observations of T Tauri mass loss tend to show much lower mass loss rates in general than are observed to be associated with the CO gas. Thus, observations have tended to show mass loss rates in the range $3 \times 10^{-9} \leq \dot{M} \leq 10^{-6}\ M_\odot\ yr^{-1}$ based on measurements of a single optical emission line. De Campli (1981) has argued that radiative driving is ruled out and that the maximum possible mass loss rate that could be driven in this system is a few times $10^{-8}\ M_\odot\ yr^{-1}$, so that the uncertainties in the measurements have badly overestimated the wind mass loss rate.

These arguments are based on the assumption that the wind arises from the T Tauri star itself. However, if there is a substantial disk around the star, then the total observed wind mass loss rates could be much higher for the very simple reason that disk surface gravity is small compared with that of the star if $M_d \ll 10^{-2}$–$10^{-3}\ M_\odot$ (see § Vc on FU Orionis phenomena). Thus, heating of a molecular disk's surface by stellar irradiation would create a substantial disk envelope, and very large mass loss rates could be driven off by the mechanism we have been discussing. The observations of an ionized outflow associated with T Tauri stars (Knapp and Padgett 1985) with $\dot{M}_w \sim 10^{-7}\ M_\odot\ yr^{-1}$ are then readily understood. Calvet, Cantó, and Rodríguez (1983) found that an optically determined $\dot{M}_* \sim 2 \times 10^{-8}\ M_\odot\ yr^{-1}$ could push the CO they observed to give their observed value of $(\dot{M}V)_{CO}$. Whether they mapped CO outflow over the size of region considered by Knapp and Padgett becomes an observational question with important consequences for these theoretical arguments.

b) Disks

Hodapp (1984) has studied the infrared polarization of the T Tauri stars HL Tau and DG Tau, as well as the infrared source SVS 13, which is believed to be the exciting star of Herbig-Haro objects 7–11. The polarization angle was observed to be perpendicular to outflow axes in all three of these objects, and is interpreted as the result of scattering of light from a central source which is heavily obscured by a disk or observed edge-on. If the polarization of field stars near these sources traces the magnetic field, then Hodapp (1984) concludes that the field is parallel to the outflow and perpendicular to an observing disk. Cohen, Harvey, and Schwartz (1985) have resolved a disklike structure of radius 5400 AU around SVS 13, and estimate that if this structure has a normal gas-to-dust ratio ($\sim$100) then its mass is $\gtrsim 0.5\ M_\odot$. Here also the disk's orientation is found to be perpendicular to the outflow direction. They also claim to marginally resolve a disk of radius $\sim$1800 AU around DG Tau, which is also perpendicular to the outflow axis. The CO map of this outflow (Snell and Edwards 1981; Bally and Lada 1983) shows a significant overlap of the velocity contours of red- and blueshifted CO gas, so that, for the disk and flow geometry under discussion, the disk would be almost face-on to the observer.

Let us predict disk mass, rotation, and density and check for consistency with flow properties. Bally and Lada (1983, hereafter BL) list the flow characteristics of HH 7–11, and these are summarized in Table 1, while the disk is taken to be $R_d = 8.1 \times 10^{16}$ cm.

TABLE 1

OBSERVED AND PREDICTED PROPERTIES OF OUTFLOWS AND MOLECULAR DISKS

PROPERTY	OBJECT[a] Orion–KL (§ Vb[i])	NGC 7538 (§ Vb[ii])	L1551 (§ Vc)	B335 (§ Vd)	HH 7–11 (SVS 13) (§ IIIb)
Observed					
E_{wind} (10^{46} ergs)	20	2	0.67×10^{-2}	2.4×10^{-2}	1.6
L_w ($L_\odot$)	2.6×10^3	1	0.2	...	6.5
L_{bol}/($L_\odot$)	2×10^4	...	25	7.6	70
M_w ($M_\odot$)	5	45	0.3	...	4.0
$(\dot{M}V)_w$ ($M_\odot\ yr^{-1}\ km\ s^{-1}$)	0.52	...	2×10^{-4}	...	4×10^{-3}
V_w (km s^{-1})	127	6.1	30	...	40
V_{rot} (km s^{-1})	2.1	4.0	0.33	...	...
R_d (10^{16} cm)	3.75	31	16	...	8.1
M_d ($10^2\ M_\odot$)	...	$\gtrsim$2.0	...	0.065 (total)	...
Predicted					
M_d ($10^2\ M_\odot$)	2.4	2.1	0.088	0.05 (assumed)	0.98
h_d ($10^{22.5}$ $cm^2\ s^{-1}$)	1.1	3.0	0.43	0.097	1.0
V_{rot} (km s^{-1})	7.8	3.1	0.88	2.2	4.1
R_d (10^{16} cm)	...	...	...	1.4	...
R_A/R_d	16	2.0	34	...	9.8
R_A (pc)	0.20	0.2	1.7	...	0.25
z_d (10^{16} cm)	0.91	7.6	3.8	...	2.0
n_d (cm^{-3})	1.5×10^9	3.2×10^5	0.51×10^7	0.73×10^9	0.7×10^8
$(M_{core}/M_\odot)/(R_{core}/10^{13.5}\ cm)$[b]	7.9	7.9	1.5	...	3.4

[a] References in parentheses are to sections of this paper.
[b] Evaluated for $\epsilon \approx 0.1$; see § IId.

The first point to note is that our theory would require that $M_d + M_* \gtrsim 4\ M_\odot$ because the high-speed CO is gas which has accelerated off the disk. Note that if the disk is being viewed nearly face-on, then the 0.5 $M_\odot$ discussed by Cohen, Harvey, and Schwartz (1985) is no real constraint on the total disk mass. If it is assumed that $E_{\rm wind} \sim E_{\rm rot}$ of the disk, then equation (3.31a) may be used together with formulae (6.1a) and (6.1b) to find that for a disk wind to drive the CO flow, it must have a mass and specific angular momentum $M_2 = 0.98$ and $h_{22.5} = 1.03$.

The scale of the outflow is in good agreement with the position of the Alfvén surface $R_{\rm A}$. Thus, a rotation of ~ 4 km s^{-1} together with an observed terminal wind speed of 40 km s^{-1} predicts, from equation (2.6), that terminal CO velocity is reached at a scale of $R_{\rm A} \approx 7.9 \times 10^{18}$ cm $= 0.25$ pc. This agrees very well with the CO data (BL) which place the high-speed lobes between 0.21 and 0.40 pc.

The observed momentum transport in the CO wind, together with $R_{\rm A}/R_d$, can be used with equation (2.17) to obtain an estimate of core properties:

$$\frac{M_{\rm core}/M_\odot}{R_{\rm core}/10^{13.5}\ {\rm cm}} = 0.34\left(\frac{0.33}{\epsilon f_g}\right). \tag{3.1}$$

As a self-consistency check, formula (3.1) may be substituted in the outflow energy equation (2.19), which results in a relation between $V_{\rm rot}$ and $(L_{\rm mech}/L_*)$. If the observed value for this ratio is used (~ 0.093), then equation (2.19) predicts $V_{\rm rot} = 2.9$ km s^{-1}, which is in good agreement with the derived value of 4.1 km s^{-1} given in Table 1.

Our theory predicts a fairly massive disk to be associated with SVS 13 and its very energetic CO outflow. Those CO outflows seen with recognizable T Tauri characteristics have energies $\sim 10^{43}$ ergs, rather than $\sim 10^{46}$ ergs, for this source.

c) *Evolution*

Since high-speed CO gas derives from an underlying molecular disk, its state in the vicinity of a young stellar object is an evolutionary indicator. When CO is very hard to detect, as is the case around many T Tauri stars, the implication is that only a disk remnant is left and that the main accretion phase is over.

Consider also the VLA radio and optical jets. According to the discussion in § II*g* and Figure 2, as the molecular outflow from a disk dies down, it is easier to see or maintain the ionized gas in the core outflow. Thus, extended-jet–like ionized-gas outflows ought to be more visible in the latter stages of disk evolution when accretion is nearly over and the molecular wind no longer obscures or forces the recombination of ionized core gas.

As the mass of the protostellar core grows relative to the remaining disk mass, the inner disk becomes Keplerian. Such a structure may be prone to instabilities (§ IV), giving outbursts similar to FU Orionis phenomena (§ V).

Herbig (1977) argued that eruptions of the FU Orionis type are repetitive and recur in the average T Tauri star after roughly 10^4 years. The known objects reached peak luminosities of $\lesssim 10^3\ L_\odot$ and sustained this maximum for a range of 11 (V1515 Cyg) to 41 (FU Ori) years. Evidence suggests that a strong wind is present during the eruptive phase. In addition, the eruptions are accompanied by apparent changes in the star in the sense that spectra at maximum and minimum are completely different, while a continuous change in the apparent spectral type of the star occurs as the star fades. The infrared excess observed during outburst could arise as a result of reprocessing of UV photons by a dusty disk.

Recent work by Hartmann and Kenyon (1985) suggests that accretion disk instability produces FU Orionis–type outbursts, as in the source V1057 Cyg. Larson (1983) has suggested that FU Orionis–type outbursts could result from runaway accretion of the inner part of a residual disk, initiated when friction heating of a protostar's outer envelope causes it to expand rapidly.

IV. HYDROMAGNETIC WINDS FROM SLOW AND FAST MAGNETIC DISK ROTORS

If winds transport disk angular momentum, there is a feature of accretion disk flows onto central objects that implies a possible two-regime structure for magnetized disks. Most of a disk's angular momentum, mass, and rotational energy resides in its outer parts, while most of its thermal energy is released in its innermost regions, where the gravitational binding energy is greatest. The magnetic flux is generally concentrated with mass, and therefore the Poynting flux originates primarily from its outer regions. Thus, the outer disk loses primarily rotational energy, whereas the flux of thermal energy comes primarily from the inner region.

Winds from the inner disk can be thermally driven (additional magnetic acceleration is not important). When this happens, this portion of the disk will be called the slow magnetic rotator (SMR) zone (see § II*a*). Winds originating from the outer disk may be Poynting flux–dominated and called the fast magnetic rotator (FMR) zone. Given a particular rotation curve and distribution of magnetic flux, a single disk may be comprised of an inner SMR and an outer FMR zone from which winds are driven by different mechanisms.

The accretion rates driven through those two zones will be different in general because FMR torques are larger than SMR torques for the same wind mass loss rate. Thus, a high mass accretion rate which is driven through the outer FMR regime encounters the inner SMR zone, which results in a mass pileup. Therefore, unsteady accretion through the inner disk is a basic feature. Outbursts in massive magnetized disks may have a dynamical basis, in contrast to a thermal instability model (e.g., Faulkner, Lin, and Papaloizou 1983). In this section, we show that with a plausible distribution of magnetic flux, various rotation curves for the disk lead to structures of the SMR–FMR or exclusively FMR type.

Let us record the properties of hydromagnetic winds close to the disk. Inside the slow point r_s of a hydromagnetic wind (i.e., in region $r_0 \le r \le r_s$), the magnetic field is primarily poloidal, and it enforces rigid corotation of the gas. Thus, $(v_p/A_p) \ll 1$ implies that $(A_\phi/A_p) \ll 1$ and $v_\phi \sim \Omega r$ in this region of the wind. The poloidal outflow speed at this point is of the order of the sound speed $v_{p,s} = s$. The exact position of r_f depends upon the importance of rotation, since, for dominant thermal effects, $r_s/r_0 \sim \psi_0/2s^2$, which is the position of the Parker critical point, while if rotation dominates thermal speeds, then $r_s/r_0 = 1/\beta^{2/3}$ where $\beta^2 \equiv (\Omega r_0)^2/\psi_0$ and

ψ_0 is the gravitational potential energy at the reference (disk) surface (see PN for the generalization of these results to non–monopolar-type geometries for the field).

The energy equation along this section of the wind outflow is easily found, since the combination of equations (2.1), (2.2), and (2.4) with $v_\phi \sim \Omega r$ allows the Poynting flux term in equation (2.1) to be approximated as $-(\Omega r)A_p A_\phi/v_p \sim [\Omega^2 r_A^2 - (\Omega r)^2]$, so that

$$E \sim \frac{1}{2} v_p^2 - \frac{1}{2}(\Omega r)^2 + \frac{1}{\gamma - 1} s^2 - \psi + \Omega^2 r_A^2 \tag{4.1}$$

is the result.

a) The FMR Regime

In all the work discussed in PN and in § II of this paper, it was assumed that the entire disk, with its centrifugally driven wind, was in an FMR regime. In order to evaluate the torque exerted upon the disk by the outflowing wind, it is necessary to find where the Alfvén surface of the wind is in the FMR regime by evaluating the energy integral E at the fast critical point, r_f. Numerical solution of equatorial wind equations (Belcher and MacGregor 1976) shows that in the FMR regime, $r_f \gg r_s, r_A$. This being the case, the poloidal outflow speed at r_f is much larger than the poloidal field Alfvén speed; $V_{r_f} \gg A_{r_f}$, and the toroidal component of the wind speed is small ($v_{\phi,f} \ll \Omega r_f$). These results reduce the field equation (2.3) to $A_\phi/A_p \sim -(\Omega r)/v_p$. At the critical point r_f, moreover, the equation of motion shows that $v_p \sim A_\phi$, so that $V_{p,f} \sim V_M$. The Poynting flux term in the energy integral (2.1) is then $V_M^3/v_{p,f} \sim V_M^2$ so that evaluating E at r_f results in

$$E = \frac{3}{2} V_M^2 + \frac{s_f^2}{\gamma - 1} - \psi_f , \tag{4.2}$$

where we recall that the rotational term $v_{\phi,f}^2$ is very small compared with the term on the right-hand side of equation (4.2).

The Alfvén radius is found by equating expressions (4.2) and (4.1), where (4.1) is evaluated at the disk surface r_0. Thus, the lever arm formula is

$$\left(\frac{r_A}{r_0}\right)^2 = \frac{3}{2}\left(\frac{V_M}{\Omega r_0}\right)^2 + \frac{s_f^2 - s_0^2}{(\gamma - 1)(\Omega_0 r_0)^2} + \frac{1}{\beta^2} - \frac{1}{2}\frac{v_{p,0}^2}{(\Omega_0 r_0)^2} + \frac{1}{2} \tag{4.3}$$

where definition (4.2) has been used.

If disks are nearly in centrifugal support, the parameter β is approximately unity. Since it is possible that magnetic support of self-gravitating disks is important, β need not necessarily be exactly unity. The dominant term in equation (4.3) for FMRs is the Poynting flux term, so that $(r_A/r_0)^2 \sim (3/2)(V_M/\Omega_0 r_0)^2$. We must immediately state that this result pertains only to equatorial winds. Geometric factors arise for polar winds (which are discussed in § II*a*) but it is anticipated that the same scaling would hold between the relevant physical quantities. Only order-unity corrections to equation (4.3) arise from polar outflows of modest opening angles. Substitution of definition (2.5) for V_M gives

$$\left(\frac{r_A}{r_0}\right)^2 \sim \left(\frac{\dot{M}_c}{\dot{M}_w}\right)^{2/3} , \tag{4.4}$$

where the characteristic wind mass loss rate $\dot{M}_c$ is

$$\dot{M}_c \equiv \left(\frac{3}{2}\right)^{2/3} \frac{\Phi^2}{\Omega r_0^3} . \tag{4.5}$$

The result in formula (4.4) suggests that $\dot{M}_c$ represents a critical wind mass loss rate such that, for a disk with $\dot{M}_c$ much less than its wind mass loss rate ($\dot{M}_w \gg \dot{M}_c$), we must be in an SMR–type regime, while $\dot{M}_w \ll \dot{M}_c$ would be an FMR regime. $\dot{M}_c$ is related to a critical accretion rate by virtue of the angular-momentum equation (2.13). Thus, using equation (2.13) to eliminate $\dot{M}_w$ in favor of $\dot{M}_a$ in (4.4) results in

$$\frac{r_A}{r_0} = \frac{\dot{M}_c}{\dot{M}_a} . \tag{4.6}$$

Thus, if $\dot{M}_a$ is regarded as being the rate at which matter is arriving at the outer edge of the disk, then if the disk is in such a state that $\dot{M}_c \gg \dot{M}_a$, an FMR regime is in order. For $\dot{M}_c$ much below $\dot{M}_a$, it is expected that an SMR state would occur.

The statements of the preceding paragraph are made precise by noting that, in the FMR zone, $V_M \gg V_P$. Thus, there is a critical condition which separates FMR and SMR zones, which is simply $(V_M/V_P)_{cr} = 1$. Writing $V_M/V_P = (V_M/\Omega_0 r_0)(\Omega_0 r_0/V_P)$ and then applying formula (2.8), there is a specific distance on the disk, $r_0 = r_t$, at which the transition between zones occurs, given by

$$\left(\frac{r_A}{r_0}\right)^2 = 3\left[\frac{1}{\gamma - 1}\left(\frac{S_0}{\Omega_0 r_0}\right)^2 + \frac{1}{2}\left(\frac{v_{p,0}}{\Omega_0 r_0}\right)^2 - \frac{1}{\beta^2}\right] = \frac{3}{2}\left(\frac{V_P}{\Omega_0 r_0}\right)^2 . \tag{4.7}$$

This result defines the transitional wind mass loss rate (at $r_0 = r_t$),

$$\dot{M}_{w,t} = \left(\frac{2}{3}\right)^{3/2}\left(\frac{\Omega_0 r_0}{V_P}\right)^3 \dot{M}_c , \tag{4.8}$$

such that when $\dot{M}_{w,t}$ is larger than the disk wind loss rate $\dot{M}_w$, then this zone is an FMR. Equivalently, a transitional accretion rate (at $r_0 = r_t$),

$$\dot{M}_{a,t} = \left(\frac{2}{3}\right)^{1/2}\left(\frac{\Omega_0 r_0}{V_P}\right)\dot{M}_c \,, \tag{4.9}$$

is defined such that when $\dot{M}_{a,t}$ is larger than the accretion rate $\dot{M}_a$ being supplied to the outer disk edge, the region is in an FMR state. This distance r_t is found by setting $\dot{M}_{a,t} = \dot{M}_a$ in equation (4.9) so that the defining equation is, at $r_0 = r_t$,

$$\left(\frac{2}{3}\right)^{1/2}\left(\frac{\Omega_0 r_0}{V_P}\right)\dot{M}_c = \dot{M}_a \,. \tag{4.10}$$

This is, in general, a complicated equation for r_t. There is a very simple case to solve, however, and that is when

$$\Omega_0 r_0/V_P = \text{const} \equiv \mathrm{K} \,. \tag{4.11}$$

One case where this might arise is that of a slablike disk with a flat rotation curve. As long as the corona above such a disk has constant thermal properties extending over the whole surface, then $V_P \sim$ constant.

b) Simple Model Examples

To proceed, we become more specific about how the magnetic flux Φ varies across the disk surface. (Note: poloidal flux is conserved *along* a set of wind flux tubes.) Blandford and Payne (1982) assumed a simple scaling of the poloidal field Alfvén velocity with the Keplerian velocity across the surfaces of a (Keplerian) accretion disk, resulting in $b_z r^2 \propto r^{3/4}$. This model then suggested that magnetic collimation of disk winds would occur because of flux concentration on the outer reaches of the disk. With this scaling, it is readily seen that from equation (4.5), $\dot{M}_c =$ const, so that the whole disk is either FMR or SMR if K is a constant. The Blandford-Payne model is self-similar even in our theory, the entire disk being either SMR or FMR.

We develop another scaling of Φ based on global (virial theorem) analysis of rotating, magnetized disks. For an equilibrium configuration of a rotating, magnetized sphere, Mestel and Paris (1979) show that Φ can be found in terms of the mass $M(r)$ and the rotation parameter β^2. For a disk the same type of result will hold, except that a different geometric factor will occur in the result. Thus, Φ is represented as

$$\Phi^2 = kGM_d^2(1 - \beta^2) \,, \tag{4.12}$$

where k is the relevant geometric factor ($k = 12/5$ for spheres and $9\pi^2/10$ for sheets) for a disk. Equation (4.12) will define the scaling relation between magnetic flux and disk mass which will be the basis of our simple model example.

Substitution of the model (4.12) into equation (4.5) for the characteristic wind mass loss rate $\dot{M}_c$ results in

$$\dot{M}_c = \left[\left(\frac{3}{2}\right)^{2/3} k\left(\frac{1}{\beta^2} - 1\right)\right] M_d \Omega \,. \tag{4.13}$$

The dependence of $\dot{M}_c$ upon β is clear in this result, because if there is no magnetic flux at all, then $\beta = 1$, which implies $\dot{M}_c = 0$ and $r_A = 0$.

The critical rate $\dot{M}_c$ is also $\dot{M}_c \propto V_\phi^3/G$ (using the definition of β^2), and the critical condition (4.10) for the determination of the critical radius evaluated at $r_0 = r_t$ is

$$\dot{M}_a = \gamma(V_0^3/G) \,, \tag{4.14}$$

where

$$\gamma \equiv \left(\frac{3}{2}\right)^{-1/6} \frac{kK}{\beta^2}\left(\frac{1}{\beta^2} - 1\right) \qquad \text{and} \qquad V_0 \equiv \Omega r_0 \,.$$

For a nearly centrifugally supported disk ($\beta \approx 1$), $\gamma \ll 1$ and the inflow is a tiny fraction of a gravitational infall.

If we denote r_d as the disk's outer radius and $X_t \equiv r_t/r_d$, $V_d \equiv V_0(r = r_d)$, then equation (4.14) may be used to find X_t in this simple case. These are (1) rigid-body rotation ($\Omega =$ const),

$$X_t = (G\dot{M}_a/\gamma V_d^3)^{1/3} \,; \tag{4.15a}$$

(2) Kepler rotation, for which

$$X_t = (\gamma V_d^3/G\dot{M}_a)^{2/3} \,; \tag{4.15b}$$

and (3) flat rotation ($V_0 =$ const), which gives no transition radius and

$$\begin{aligned} G\dot{M}_a/\gamma V_d^3 &\geq 1 \quad \text{(SMR)} \\ &\leq 1 \quad \text{(FMR)} \,. \end{aligned} \tag{4.15c}$$

Consider the case of the protostellar disk analyzed in § II*c*. For massive star formation in Orion-like systems, equation (4.15b) gives

$$X_t = 0.32\gamma^{-1/3}(\dot{M}_a/10^{-4}\ M_\odot\ \mathrm{yr}^{-1})^{1/3}(V_d/10^{5.5}\ \mathrm{cm\ s}^{-1})^{-1} \,.$$

Therefore, if the inner portions of Orion-like molecular disks behave like rigid rotors, then a large SMR zone could lie between the protostellar surface and the strongly torqued outer portions of the disk. Since the massive bipolar outflow is predicted to begin on scales $r \gtrsim 10^{15}$ cm, however, a self-consistent picture requires the disk around IRc2 to have $V_\phi = \text{const}$. It is to be hoped that high-resolution observations will soon be able to test this.

c) *The SMR Zone*

A thermal wind possesses only a small lever arm, or $r_A(r) \approx r$, so that the steady state angular-momentum equation (2.13) may be applied to give $\dot{M}_w \sim \dot{M}_a$. This suggests that a good fraction, if not most, of the mass entering into an SMR region would have to be pumped into the wind if a steady state accretion flow were to be driven into the central objects.

V. A WIND THEORY FOR FU ORIONIS PHENOMENA

a) *Nonsteady Behavior of Disks with Inner SMR Zones*

The inefficiency of thermally driven winds in conveying angular momentum makes a steady state disk with an interior SMR zone, in general impossible. This is seen by the following argument. If $\dot{M}_{a,f}$ and $\dot{M}_{a,s}$ represent the accretion rates being driven through the FMR and SMR zones, respectively, then continuity demands

$$\dot{M}_{a,f} = \dot{M}_{a,s} + \dot{M}_{w,s} , \tag{5.1}$$

where $\dot{M}_{w,s}$ is the wind mass loss rate in the SMR zone. However, if steady state evolution is supposed, then $\dot{M}_{a,f} \sim \dot{M}_{a,s}$. The contradiction arises when it is noted that the inefficiency of SMR torques always gives $\dot{M}_{a,s} \sim \dot{M}_{w,s}$, so that equation (5.1) cannot be satisfied. A steady state disk can occur when the magnetic flux and angular-momentum distributions are such that the entire disk is FMR. Disks possessing inner SMR zones have transient behavior in order to solve the accretion problem.

b) *Outbursts from Two-Zone Disks*

Because of the inefficiency of SMR torques at removing angular momentum, disks which possess inner SMR zones pile up mass at the transition radius r_t between SMR and FMR regions. This is a situation reminiscent of the mass storage models for cataclysmic variables, as analyzed by Osaki (1974) and Smak (1984). Mass accumulation can drive the reservoir into various types of instabilities, many of which could be important in forcing blobs to get down to the central object's surface.

For example, one possible type of mechanism involves the accumulation of mass in a reservoir until its self-gravitation becomes important. A disk with rigid body or with Keplerian rotation has an inner SMR zone, while $V_\phi = \text{const}$ would be completely FMR. Mass accumulation could slowly alter the rotation curve in the inner region, flattening it into a $V_\phi = \text{const}$ law. Once the inner region is converted into an FMR, an outburst must develop as dense disk material is driven onto the central object. The heating results in large wind mass loss rates from the disk, which, in turn, drives more accretion and more heating. The runaway shuts off when the mass reservoir has become sufficiently depleted of mass by wind and large accretion losses.

The maximum accumulation time scale which precedes outburst spans a large range of dynamical time scales in the disk, depending upon the amount of magnetic flux which threads the disk. The largest disk surface density achievable before instabilities set in is (at $r_0 = r_t$)

$$\Sigma_{cr} = \frac{\lambda}{Q} \frac{c_d \Omega}{\pi G} , \tag{5.2}$$

where Q here is taken to be of order unity and the region around r_t is the site of the accumulating gas mass. Now, gas is being drained from the outer disk by the inefficiently operating FMR torque, driving an accretion rate at $\dot{M}_a$. The critical time required to accumulate the surface density (5.2) is of order $t_{cr} \approx (\pi r_t^2 \Sigma_{cr} - \dot{M}_a)$.

Let us specialize to the case where the SMR zone is rigidly rotating. The use of the critical condition (4.20) with equation (5.2) yields, at $r_0 = r_t$,

$$t_{cr} \Omega \approx \frac{\lambda}{Q} \frac{1}{\gamma} \left(\frac{c_d}{V_0} \right) , \tag{5.3}$$

where the subscript t merely denotes the evaluation of quantities at the transition radius r_t. It should be remembered that equation (5.3) holds only for our magnetic flux scaling with the disk mass. When a significant flux threads the disk ($\beta^2 \lesssim \frac{1}{2}$, say), and here we are specifically considering the protostellar case, γ is approaching unity and the critical time scale becomes of the order of the dynamic time Ω^{-1}. The point is that, in this limit, the large magnetic flux drives a large accretion rate.

When the disk's own surface gravity begins to exceed the vertical component of the central object's gravitational force, which implies that with $g_s = 2\pi G \Sigma$, the critical density will be given as $\Sigma_{cr} \approx M_{core} z_t / 2\pi r_t^3$), where M_{core} is the central object's mass, and we evaluate the various quantities at the transition radius. Clearly, then, when self-gravitation is important,

$$\frac{M_d}{M_{core}} \approx \frac{z_d}{r} , \tag{5.4}$$

where the disk mass at r_t is estimated as $M_d \equiv 2\pi \Sigma_{cr} r_t^2$. This cold mass reservoir in the disk will have $M_d \approx (10^{-1}\text{–}10^{-2}) M_{core}$ of material accumulated at the outset of an outburst. The time to outburst is of order

$$t_{cr} \approx \frac{z_d}{r} \frac{M_{core}}{\dot{M}_a} , \tag{5.5}$$

where quantities are evaluated at r_t.

Finally, the coefficient γ is found if formula (5.5) is compared with formula (5.3). Since r_t marks the boundary between a fairly massive outer FMR zone and the sparse SMR region, then $z_d/r \sim c_d/V_0$ at $r = r_t$, so that

$$\gamma \approx \frac{Q}{\lambda} \frac{\dot{M}_a}{M_{\rm core}\Omega_t} . \tag{5.6}$$

For a large core mass $M_{\rm core}$, γ is expected to be tiny, which from equation (4.22) shows that $\beta \approx 1$.

c) *The FU Orionis Phenomenon as Feeding from a Remnant Disk*

We propose that the FU Orionis type of outburst arises from the accretion of mass from a self-gravitating portion of a surrounding molecular disk which is the fairly evolved remnant of material out of which the T Tauri star formed. The eruption begins as the mass reservoir reaches a surface density which makes it self-gravitating and unstable, perhaps in the sense of § V*b*.

The outburst luminosity stems from the accretion of material from the disk, mass reservoir, and onto the protostellar core, producing

$$L_{\rm outburst} = \frac{G\dot{M}_a M_{\rm core}}{R_{\rm core}} \approx 4.1 \times 10^{36} \left(\frac{M_{\rm core}}{M_\odot}\right)\left(\frac{R_{\rm core}}{10^{12.5}\ {\rm cm}}\right)^{-1}\left(\frac{\dot{M}_a}{10^{-3}\ M_\odot\ {\rm yr}^{-1}}\right) {\rm ergs\ s}^{-1} . \tag{5.7}$$

Thus, an accretion rate of $\dot{M}_{a,\rm outburst} \sim 10^{-3}\ M_\odot\ {\rm yr}^{-1}$ gives the observed outburst luminosity of $10^3\ L_\odot$. For an outburst lasting 40 years (FU Ori) the implied total mass in the reservoir is $M_d \approx (\dot{M}_a t)_{\rm outburst} \approx 4 \times 10^{-2}\ M_\odot$. This mass is very close to the estimate following formula (5.4) of the maximum mass expected in the disk reservoir at $r \sim r_t$ and suggests that self-gravitation plays a role. The time scale between bursts is the time required for a disk evolving under FMR torques to accumulate a mass M_d at the accretion rate $\dot{M}_{a,\rm quiet}$. For $t_{\rm cr} \sim 10^4$ yr, this means $\dot{M}_{a,\rm quiet} \approx 4 \times 10^{-7}\ M_\odot\ {\rm yr}^{-1}$. This quiet accretion rate is precisely the steady state rate that would build a low-mass star, which is consistent with having a T Tauri star as the central object. Our theory demands that this quiescent accretion rate is driven by a more tenuous disk wind. The prediction is that during the quiescent phase, an FU Orionis object blows off a disk wind with $\dot{M}_{w,\rm quiet} \lesssim 10^{-7}\ M_\odot\ {\rm yr}^{-1}$, which goes well with the observation of T Tauri star wind mass loss rates in general.

VI. PREDICTIONS AND OBSERVATIONAL TESTS

a) *Energetics*

The energy reservoir of the magnetically driven outflow is the rotational energy of the disk. The magnetic field is the means by which this rotational energy may be extracted from the disk and transported out to infinity. For a rigidly rotating disk, the energy reservoir for a disk of radius R_d is

$$E_{\rm rot} = 1.80 \times 10^{46} M_2^3 h_{22.5}^{-2}\ {\rm ergs} , \tag{6.1a}$$

$$R_d = 7.5 \times 10^{16} M_2^{-1} h_{22.5}^2\ {\rm cm} . \tag{6.1b}$$

where the normalizations appropriate to molecular disks are taken as $M_2 \equiv (M/100)\ M_\odot$ and $h_{22.5} \equiv h/10^{22.5}\ {\rm cm^2\ s^{-1}}$. Relations (6.1) assume that the outer edge of the disk is centrifugally supported. If the bipolar flows carry off disk rotational energy, then $E_{\rm wind} \sim E_{\rm rot}$ above, so that $E_{\rm wind}$ can be used together with an observed rotation curve to predict the disk mass that must be present. We will illustrate this in concrete examples to follow.

b) *Massive Star Formation*

i) *Orion–KL*

A strong test for the presence of molecular disks is the high-resolution interferometric work being done with the facilities at Hat Creek and Owens Valley. It has been discovered that a dense disk surrounds IRc2 in the Kleinmann-Low nebula, which extends outward at least 2500 AU (Vogel *et al.* 1985; Plambeck *et al.* 1985) and to within at least 35 AU of the central infrared source. There is no evidence for a highly collimated outflow at IRc2. Instead, maps of the extreme line wings of SiO in the immediate vicinity of IRc2 remain relatively extended on scales corresponding to that of the disk (Plambeck *et al.* 1985), providing evidence for a wind which originates from the disk surface as a centrifugally driven hydromagnetic outflow. The appearance of an apparent high-speed (i.e., 30–40 km s^{-1}) component at the disk surface is, in this model, a projection effect. If the outflow is inclined to the observer, then the highest speed neutral gas (which is accelerated off the outer portions of the disk) will be projected against the disk surface in a way that the observations seem to show. The outflow itself is one of the most poorly collimated of all the high-speed flows on BL's list.

The observations of the wind are summarized (BL) and given in Table 1, where the disk is resolved at $R_d = 2500$ AU $= 3.75 \times 10^{16}$ cm. By the procedure of § III, the use of formulae (6.1), and the wind observations the predictions for disk properties are obtained, and are listed in Table 1.

Plambeck *et al.* (1985) note that the disk is inclined at perhaps 40°. Thus, while the observed rotation is at 2.1 km s^{-1}, our calculated rotation of 7.8 km s^{-1} requires an inclination of 15°. Inclination of the disk is crucial to determine the rotation and hence the dynamical mass. The outflow is poorly collimated, and no large error is made in the estimates of wind energetics. The rotation speed is predicted for the disk based on equation (2.19) and $(L_{\rm mech}/L_*) \approx 0.13$ predicts $V_{\rm rot} \approx 5.4$ km s^{-1}, which shows reasonable consistency with the method that gave our 7.8 km s^{-1} prediction. The extreme nature of the disk in formula (6.3) is a consequence of the enormous energy that the molecular outflow is observed to carry.

ii) *NGC 7538*

Recent high-resolution CO observations toward NGC 7538 have resolved a disk with a radius of ~ 0.1 pc rotating at 4 km s^{-1} (Sargent *et al.* 1985). The bipolar outflow characteristics are listed in column (2) of Table 1, as are our predictions. The rotation speed predicted for the disk based on equation (2.19) and an assumed $L_{IR} = 10^3\ L_\odot$ is $V_{rot} \approx 3.8(L_*/10^3\ L_\odot)^{1/2}$ km s^{-1}. Although there are many infrared sources in the region with a total IR luminosity of $\sim 10^5\ L_\odot$ (Werner *et al.* 1979), the source IRS 1 in question has been taken to be $10^3\ L_\odot$ for the best agreement with observations. For $L_* \sim 10^4\ L_\odot$, a rotation of 12 km s^{-1} for the disk would imply an inclination angle of $\sim 20°$ to be compatible with the observed 4 km s^{-1}. The agreement with the observed and infrared disk mass is a feature which may mean that a large effect due to viewing angle may not be relevant here.

c) Low-Mass Star Formation: L1551

Observations with the Nobeyama 45 m telescope have turned up the presence of a rotating molecular disk around IRS 5 in the cloud L1551 (Kaifu *et al.* 1984). The reported disk is on a scale of $R_d \sim 0.05$ pc and a rotation frequency of $\Omega \sim 2.2 \times 10^{-13}$ s^{-1}, corresponding to a rotation speed of $V_{rot} \sim 0.33$ km s^{-1}.

The observation of the outflow summarized in BL are listed in column (3) of Table 1, while the disk is taken to be resolved at $R_d \approx 0.05$ pc $= 1.55 \times 10^{17}$ cm. We caution that if a smaller, more rapidly rotating core is found, then the predictions of the model change. From the observed energy of flow and disk radius, our procedure yields the predictions given in Table 1. The rotation speed predicted for the disk, based on equation (2.19) and $(L_{mech}/L_*) \approx 0.8 \times 10^{-2}$, gives $V_{rot} \approx 0.57$ km s^{-1}.

d) Outflows in Bok Globules

The study of bipolar outflows and star formation in Bok globules promises to be extremely important because these dark clouds are isolated, nearby in some cases, and seem to be forming only one or two stars. The finding of Keene *et al.* (1983) that a pointlike source of 7.6 $L_\odot$ is present inside the globule B335 indicates that star formation is occurring in this cloud. Recent observations of the $J = 1$–0 transition of ^{1} CO and ^{13}CO (Goldsmith *et al.* 1984) have turned up the presence of bipolar molecular outflows which have $\dot{M}_w V_w/(L/c) \sim 500$ (note—this in spite of $L/L_{mech} \sim 250$). If the observations of B335 are considered (Goldsmith *et al.* 1984), a total of (0.1–2.44) $\times 10^{44}$ ergs at a mass loss rate of (0.3–7.5) $\times 10^{-7}\ M_\odot$ yr^{-1} is estimated (lower limits do not include geometric and optical depth corrections, while upper limits do). The wind speed is of order 4.0 km s^{-1}. This small outflow speed cautions one not necessarily to lump this supposed outflow with the class of objects with $V_w \geq 10$ km s^{-1}.

A constraint arises from the infrared observations. On the basis of the 400 μm optical depth, Keene *et al.* (1983) were able to derive a core mass for the system of $\sim 6.5\ M_\odot\ (D/400$ pc).

In the present absence of observations of a resolved disk at the heart of this outflow, we guess that a star of mass $M \lesssim M_\odot$ is forming in the globule. A reasonable estimate of disk mass may then be $M \lesssim 5\ M_\odot$. This, taken together with the outflow of 2.4×10^{44} ergs, allows us to make the estimates in column (4) of Table 1.

e) A Concrete Test of the Acceleration Mechanism

We propose a very specific test of the centrifugal wind drive for bipolar molecular outflows. This test is best carried out for well-resolved molecular outflows such as those in Orion–KL and L1551, and high-resolution interferometric work done on the high-velocity wings of lines is optimal. The point about winds in this theory is that they corotate with the underlying disk out to about the wind Alfvén radius. Thereafter, V_ϕ decreases as r^{-1}, so that the poloidal outflow becomes entirely dominant (see discussion in § III*a*). Thus, maps made in some molecule which is sure to be a tracer of the accelerating gas should show some *characteristic of rotation about to the flow axis out to a distance* r_A (see Fig. 1). The reason for this is that, as the gas is accelerated up to high poloidal speed, it is also forced to corotate with the underlying disk. We regard this as a definitive test of the acceleration mechanism. In effect, then, one could experimentally determine the angular-momentum transport rate by the wind. If this could be achieved, every aspect of the theory would be open to observational test.

VII. CONCLUSIONS

The main conclusions we draw about the action of hydromagnetic disk winds are as follows:

1. Disk winds drive accretion rates of order $\dot{M}_a \sim (R_A/R_d)^2 \dot{M}_w$, so that massive bipolar molecular outflows may indicate the main accretion phase during star formation with disks. Such winds can also solve the angular-momentum problem of star formation.

2. Assuming that the infrared luminosity of embedded protostellar cores is due to accretion, it can be shown that hydromagnetic disk torques account for both the momentum balance $[(\dot{M}V)_w \gtrsim (10^2$–$10^3)(L_*/c)]$ and the energetics ($L_{mech}/L_* \lesssim 10^{-2}$ typically) observed for bipolar outflows.

3. Accretion onto a protostellar core always produces a two-component outflow: an ionized-gas outflow on scales $R^I_{en} \lesssim 10^{15}$ cm, $\dot{M}_{ion} \sim 10^{-6}\ M_\odot$, and $V_{ion} \sim 250$ km s^{-1} (these values for massive disks with $V_\phi = $ const) and a molecular outflow on scales 10^{15} cm $\lesssim r \lesssim 10^{17}$ cm, with $\dot{M}_{molec} \approx 10^{-4}\ M_\odot$ yr^{-1} and $V_{molec} \sim 50$ km s^{-1}.

4. VLA and optical jets are predicted to be the thermal cores of the much more extensive molecular outflow. Jetlike features develop at the end of the massive bipolar flow epoch.

5. Herbig-Haro objects are associated with the core outflow. They may arise by Kelvin-Helmholtz instability between the fast-moving inner flow, and the outer, slower molecular flow.

6. FU Orionis–type outbursts may develop from disks when protostellar cores grow massive enough that an inner Keplerian or rigid-body regime (SMR) grows in a disk which has $V_\phi = $ const (FMR) in its outer parts. Mass piles up at the boundary of these two regimes because higher accretion rates are driven by FMR than by SMR winds. A 10^4 yr burst time scale corresponds to the time scale for which this reservoir grows to be self-gravitating.

7. Detailed predictions of disk and flow characteristics have been made (§§ V*b*, V*c*, III*b*, and V*d*). As an example, disk masses and rotations are as follows: *Orion–KL*: 237 $M_\odot$, 7.8 km s^{-1} (disk inclined at $\sim 15°$). *NGC 7538*: 214 $M_\odot$, 3.1 km s^{-1}; *L1551*: 8.8 $M_\odot$, 0.88 km s^{-1}; *HH 7–11 (SVS 13)*: 98 $M_\odot$, 4.1 km s^{-1}; *B335*: 5 $M_\odot$, 2.2 km s^{-1}; and radius $R_d \approx 1.4 \times 10^{16}$ cm.

8. A direct observational test for the acceleration mechanism which distinguishes centrifugal winds is to look for line asymmetry in outflowing (red- and blueshifted) gas, characteristic of rotation.

9. Lobes of high-speed CO emission are scales ($\sim R_A$) at which molecular gas, accelerated from an underlying molecular disk, reaches terminal speed. A full range of intermediate-velocity gas is spatially distributed between these lobes and the disk. Swept up ambient material lies in a shell between the regions of CO and H_2 emission.

10. The derivation of the hydromagnetic wind torque is general, and application to other accreting systems with winds and jets is possible.

It is a pleasure to thank Martin Cohen, Lee Hartmann, Arieh Königl, Julian Krolik, Richard Plambeck, Anneila Sargent, Steven Shore, Joseph Silk, and Stuart Vogel for informative and stimulating discussions, and an anonymous referee for useful remarks. R. E. P. thanks Space Telescope Science Institute and colleagues at Johns Hopkins for their kind hospitality. This research was supported by the Johns Hopkins University.

REFERENCES

Bally, J., and Lada, C. J. 1983, *Ap. J.*, **265**, 824 (BL).
Begelman, M. C., McKee, C. F., and Shields, G. A. 1983, *Ap. J.*, **271**, 70.
Belcher, J. W., and MacGregor, K. B. 1976, *Ap. J.*, **210**, 498.
Bieging, J. H., Cohen, M., and Schwartz, P. R. 1984, *Ap. J.*, **282**, 699.
Blandford, R. D., and Payne, D. R. 1982, *M.N.R.A.S.*, **199**, 883.
Calvet, N., Cantó J., and Rodríguez, L. F. 1983, *Ap. J.*, **268**, 739.
Cohen, M., Bieging, J. H., and Schwartz, P. R. 1982, *Ap. J.*, **253**, 707.
Cohen, M., Harvey, P. M., and Schwartz, R. D. 1985, *Ap. J.*, **296**, 633.
Cohen R. J., Rowland, P. R., and Blair, M. M. 1984, *M.N.R.A.S.*, **210**, 425.
DeCampli, W. M. 1981, *Ap. J.*, **244**, 124.
Draine, B. T. 1983, *Ap. J.*, **270**, 519.
Draine, B. T., and Roberge, W. G. 1982, *Ap. J. (Letters)*, **259**, L91.
Edwards, S., and Snell, R. L. 1984, *Ap. J.*, **281**, 237.
Faulkner, J., Lin, D. N. C., and Papaloizou, J. C. B. 1983, *M.N.R.A.S.*, **205**, 359.
Goldsmith, P. F., Snell, R. L., Hemeon-Heyer, M., and Langer, W. D. 1984, *Ap. J.*, **286**, 599.
Hartmann, L., and Kenyon, S. J. 1985, *Ap. J.*, submitted.
Hartmann, L., and MacGregor, K. B. 1982, *Ap. J.*, **259**, 180.
Herbig, G. H. 1977, *Ap. J.*, **217**, 693.
Hodapp, K. W. 1984, *Astr. Ap.*, **141**, 255.
Jones, T. J., Hyland, A. R., and Bailey, J. 1984, *Ap. J.*, **282**, 675.
Kaifu, N., *et al.* 1984, *Astr. Ap.*, **134**, 7.
Keene, J., Davidson, J. A., Harper, D. A., Hildebrand, R. H., Jaffe, D. T., Loewenstein, R. F., Low, F. J., and Pernic, R. 1983, *Ap. J. (Letters)*, **274**, L43.
Knapp, G. R., and Padgett, D. L. 1985, *Ap. J.*, preprint.
Königl, A. 1982, *Ap. J.*, **261**, 115.
Larson, R. B. 1983, *Rev. Mexicana Astr. Ap.*, **7**, 219.
Lüst, R. 1952, *Zs. Naturforschung*, **7a**, 87.
Lynden-Bell, D., and Pringle, J. E. 1974, *M.N.R.A.S.*, **168**, 603.
Mestel, L. 1968, *M.N.R.A.S.*, **138**, 359.
Mestel, L., and Paris, R. B. 1979, *M.N.R.A.S.*, **187**, 337.
Michel, F. C. 1969, *Ap. J.*, **158**, 727.
Mundt, R., and Fried, J. W. 1983, *Ap. J. (Letters)*, **274**, L83.
Mundt, R., and Hartmann, L. 1983, *Ap. J.*, **268**, 766.
Osaki, Y. 1974, *Pub. Astr. Soc. Japan*, **26**, 429.
Panagia, N., and Felli, M. 1975, *Astr. Ap.*, **39**, 1.
Plambeck, R. L., Vogel, S. N., Wright, M. C. H., Bieging, J. H., and Welch, W. J. 1985, preprint.
Pringle, J. E. 1977, *M.N.R.A.S.*, **178**, 195.
———. 1981, *Ann. Rev. Astr. Ap.*, **19**, 137.
Pudritz, R. E. 1981, *M.N.R.A.S.*, **195**, 897.
———. 1985, *Ap. J.*, **293**, 216.
Pudritz, R. E., and Norman, C. A. 1983, *Ap. J.*, **274**, 677 (PN).
———. 1986, in *Proc. Conf. on Jets from Stars and Galaxies* (Toronto, 1985 June) (*Canadian J. Phys.*, in press).
Roxburgh, I. W. 1983, in *IAU Symposium 102, Solar and Stellar Magnetic Fields: Origins and Coronal Effects*, ed. J. Stenflo (Dordrecht: Reidel), p. 449.
Sakurai, T. 1985, Preprint.
Sargent, A. 1985, in *Proc. Conf. on Masers, Molecules and Mass Outflows in Regions of Star Formation* (Haystack Observatory, 1985 May), in press.
Sato, S., Nagata, T., Nakajima, T., Nishida, M., Tanaka, M., and Yamashita, T. 1985, *Ap. J.*, **291**, 708.
Schwartz, R. D. 1983, *Ann. Rev. Astr. Ap.*, **21**, 209.
Shakura, N. I., and Sunyaev, R. A. 1973, *Astr. Ap.*, **24**, 337.
Smak, J. 1984, *Pub. A.S.P.*, **96**, 5.
Snell, R. L., and Edwards, S. 1981, *Ap. J.*, **251**, 103.
Uchida, Y., and Shibata, K. 1985, *Pub. Astr. Soc. Japan*, **37**, in press.
Ulrich, R. K., and Knapp, G. R. 1985, preprint.
Vogel, S. N. 1985, *Ap. J.*, preprint.
Vogel, S. N., *et al.* 1985, *Ap. J.*, preprint.
von Weizsäcker, C. F. 1943, *Zs. Ap.*, **22**, 319.
Werner, M. W., Becklin, E. E., Gatley, I., Matthews, K., Neugebauer, G., and Wynn-Williams, C. G. 1979, *M.N.R.A.S.*, **188**, 463.

COLIN A. NORMAN and RALPH E. PUDRITZ: Department of Physics and Astronomy, Johns Hopkins University, Homewood Campus, Baltimore, MD 21218